

## Applications of UV/Vis Spectroscopy in Characterization and Catalytic Activity of Noble Metal Nanoparticles Fabricated in Responsive Polymer Microgels: A Review

Robina Begum, Zahoor H. Farooqi, Khalida Naseem, Faisal Ali, Madeeha Batool, Jianliang Xiao & Ahmad Irfan

To cite this article: Robina Begum, Zahoor H. Farooqi, Khalida Naseem, Faisal Ali, Madeeha Batool, Jianliang Xiao & Ahmad Irfan (2018): Applications of UV/Vis Spectroscopy in Characterization and Catalytic Activity of Noble Metal Nanoparticles Fabricated in Responsive Polymer Microgels: A Review, Critical Reviews in Analytical Chemistry, DOI: [10.1080/10408347.2018.1451299](https://doi.org/10.1080/10408347.2018.1451299)

To link to this article: <https://doi.org/10.1080/10408347.2018.1451299>



Published online: 30 Mar 2018.



Submit your article to this journal [↗](#)



View related articles [↗](#)



# Applications of UV/Vis Spectroscopy in Characterization and Catalytic Activity of Noble Metal Nanoparticles Fabricated in Responsive Polymer Microgels: A Review

Robina Begum<sup>a,b,c</sup>, Zahoor H. Farooqi<sup>b</sup>, Khalida Naseem<sup>b</sup>, Faisal Ali<sup>b</sup>, Madeeha Batool<sup>b</sup>, Jianliang Xiao<sup>c</sup>, and Ahmad Irfan<sup>d,e</sup>

<sup>a</sup>Centre for Undergraduate Studies, University of the Punjab, New Campus, Lahore, Pakistan; <sup>b</sup>Institute of Chemistry, University of the Punjab, New Campus, Lahore, Pakistan; <sup>c</sup>Department of Chemistry, University of Liverpool, Liverpool, UK; <sup>d</sup>Research Center for Advanced Materials Science, King Khalid University, Abha, Saudi Arabia; <sup>e</sup>Department of Chemistry, Faculty of Science, King Khalid University, Abha, Saudi Arabia

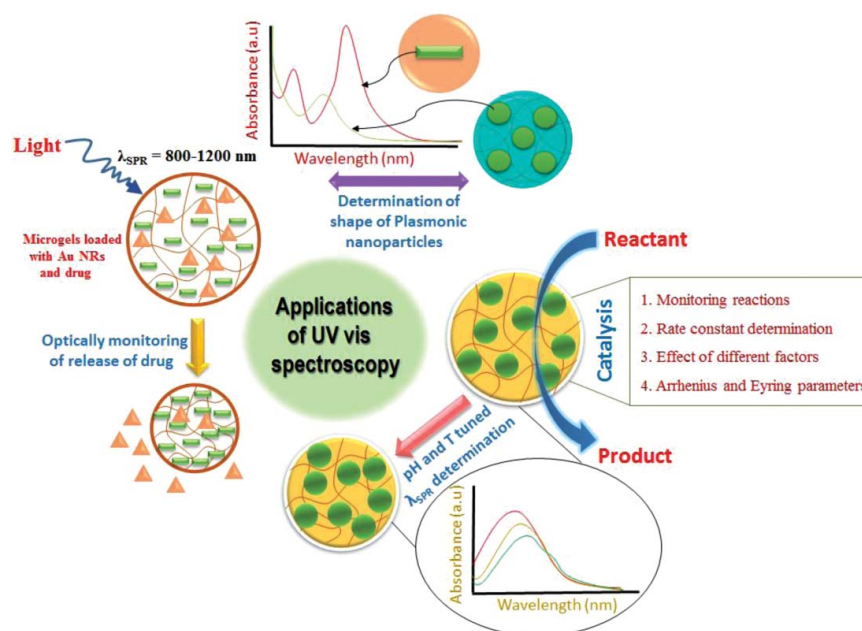
## ABSTRACT

Noble metal nanoparticles loaded smart polymer microgels have gained much attention due to fascinating combination of their properties in a single system. These hybrid systems have been extensively used in biomedicines, photonics, and catalysis. Hybrid microgels are characterized by using various techniques but UV/Vis spectroscopy is an easily available technique for characterization of noble metal nanoparticles loaded microgels. This technique is widely used for determination of size and shape of metal nanoparticles. The tuning of optical properties of noble metal nanoparticles under various stimuli can be studied using UV/Vis spectroscopic method. Time course UV/Vis spectroscopy can also be used to monitor the kinetics of swelling and deswelling of microgels and hybrid microgels. Growth of metal nanoparticles in polymeric network or growth of polymeric network around metal nanoparticle core can be studied by using UV/Vis spectroscopy. This technique can also be used for investigation of various applications of hybrid materials in catalysis, photonics, and sensing. This tutorial review describes the uses of UV/Vis spectroscopy in characterization and catalytic applications of responsive hybrid microgels with respect to recent research progress in this area.

## KEYWORDS

UV/Vis spectroscopy; plasmonic nanoparticles; hybrid microgels; applications

## GRAPHICAL ABSTRACT



## Introduction

Synthesis and characterization of noble metal nanoparticles for various applications are current areas of research.<sup>[1–4]</sup> Strategies used for their fabrication and characterization are going to be improved day by day. Control over size and shape of nanoparticles is very important for their potential applications in various fields.<sup>[5,6]</sup> Moreover, these nanoparticles are highly unstable due to their high surface energy and are converted into bulk materials as a result of their aggregation.<sup>[7, 8]</sup> Therefore, metal nanoparticles are stabilized using various stabilizing agents like surfactants,<sup>[9]</sup> dendrimers,<sup>[10]</sup> block copolymers,<sup>[11]</sup> and microgels.<sup>[12]</sup> The metal nanoparticles loaded microgels have properties of both nanoparticles and polymer microgels and are called hybrid microgels.<sup>[13]</sup> Hybrid microgels loaded with metal nanoparticles have potential to be used in biomedicine,<sup>[14]</sup> optics,<sup>[15]</sup> electronics,<sup>[16]</sup> photonics,<sup>[17]</sup> and catalysis.<sup>[18]</sup> Hybrid microgels are characterized by Transmission electron microscopy (TEM),<sup>[19]</sup> Scanning electron microscopy (SEM),<sup>[20]</sup> Atomic Force microscopy (AFM),<sup>[21,22]</sup> Dynamic light scattering (DLS),<sup>[23]</sup> X-ray diffraction (XRD),<sup>[24]</sup> Fourier transform infrared spectroscopy (FTIR),<sup>[25]</sup> and ultraviolet visible spectroscopy (UV/Vis).<sup>[26]</sup> Each technique has its own advantages and disadvantages and it is hard to compare one technique to another because each technique has a specific purpose and used to get a specific information that cannot be obtained from the other one. For example, UV/Vis spectroscopy is only one method among all above-mentioned techniques, which can be used to study the kinetics of swelling and deswelling of polymer microgels and hybrid microgels having small particle size.<sup>[27]</sup> UV/Vis spectroscopy is generally used for characterization of Plasmonic nanoparticles loaded hybrid microgels and study of their applications.<sup>[19, 24]</sup> It has been reported as an effective tool for study of tuning of optical properties of Plasmonic nanoparticles loaded into polymer microgels.<sup>[28]</sup> Catalytic activity of nanoparticles can also be studied by using UV/Vis spectroscopy.<sup>[29]</sup> Progress of catalytic reactions can be monitored by UV/Vis spectrophotometry. For example, Farooqi et al. used UV/Vis spectroscopy for characterization of silver-poly(N-isopropylacrylamide-acrylic acid) [Ag-P(NIPAM-AA)] hybrid microgels.<sup>[30]</sup> The fabrication of silver nanoparticles (Ag NPs) in P(NIPAM-AA) microgels was confirmed by surface Plasmonic resonance (SPR) peak of Ag NPs at 400 nm. They investigated the stability of Ag NPs in polymer microgels using UV/Vis spectroscopy. The tuning of optical properties of Ag NPs was also studied using same technique. Same group of researchers investigated the catalytic activity of silver-poly(N-isopropylacrylamide-methacrylic acid) [Ag-P(NIPAM-Ma)] hybrid microgels toward catalytic reduction of 2-nitroaniline (2-NA) into 2-aminoaniline (2-AA) in aqueous medium using same technique.<sup>[24]</sup> Das et al. used UV/Vis spectroscopy for investigation of growth of gold nano rods (Au NRs) synthesized by seed mediated growth method.<sup>[31]</sup> They adjusted the aspect ratios of Au NRs in such a way that they should have longitudinal SPR wavelength in water window region. UV/Vis spectroscopy was used for this purpose. Khan et al. prepared P(NIPAM-AA) microgels by microwave irradiation method and used them as micro-reactors for in-situ fabrication of Ag NPs using glucose as reducing agent.<sup>[32]</sup> Fabrication of Ag NPs in microgels network was confirmed by appearance of SPR band in UV/Vis region at 429nm. Volden et al. studied the temperature dependent optical properties of gold nanoparticles

(Au NPs) impregnated P(NIPAM) microgels by UV/Vis spectroscopy.<sup>[33]</sup> Optical properties of Au-P(NIPAM) hybrid microgels were studied at two different values of temperature (25°C and 60°C) using UV/Vis spectroscopy. Shift in optical properties of Au-P(NIPAM) hybrid microgels with increase/decrease in temperature was found to be completely reversible. Extensive use of this technique in characterization and applications of hybrid microgels stimulated us to summarize its utility in research work on this area in the last several years in the form of a review article.

Applications of UV/Vis spectroscopy in study of characterization of metal nanoparticles loaded into polymer microgels, growth of metal nanoparticles in microgels, growth of polymeric network around a metal nanoparticle core, stability of metal nanoparticles, optical properties of hybrid microgels, properties of hybrid microgels produced due to presence of inorganic and organic components in hybrid system have been discussed in detail in this review. The monitoring of catalytic reactions occurring in the presence of hybrid microgels and determination of various kinetic parameters of these catalytic reactions using UV/Vis spectroscopy has also been described in this review. Summary and future perspectives have been also presented in this review for further development in this area.

## Characterization of nanoparticles loaded into microgels by UV/Vis spectroscopy

It is well known that Plasmonic nanoparticles absorb radiations of visible to near infrared region (NIR) depending upon the size and shape of nanoparticles. This property is associated to collective oscillation of surface electrons of nanoparticles and known as SPR. Due to SPR property of nanoparticles, dispersion of Plasmonic nanoparticles gives one or more peaks that can be used to get useful information regarding shape, size and size distribution of nanoparticles. That is why, UV/Vis spectroscopy is widely used for characterization of Plasmonic nanoparticles loaded into smart polymer microgels. Farooqi et al. used UV/Vis spectroscopy for characterization of P(NIPAM-AA) microgels and Ag-P(NIPAM-AA) hybrid microgels.<sup>[19]</sup> They scanned UV/Vis spectra of dilute dispersion of pure microgels and hybrid microgels samples in the wavelength range of 200–800 nm and observed that pure microgels have no band in this region but hybrid microgels dispersion has a single narrow peak at 420 nm. They reported that single peak at specific value of wavelength (420 nm) known as SPR wavelength ( $\lambda_{SPR}$ ) indicates that spherical nanoparticles have been successfully loaded into the polymer network. The small value of full width at half-maximum is an indication of small size distribution of nanoparticles. Zhang and coworkers reported the UV/Vis analysis of cadmium sulfide (CdS) and Ag NPs loaded poly(N-isopropylacrylamide-acrylic acid-2-hydroxy ethyl acrylate) [P(NIPAM-AA-HEAc)] hybrid microgels to evaluate their optical properties for the purpose of their photonic applications.<sup>[34]</sup> Acrylic acid (AA) was copolymerized to provide functional groups for coupling with metal ions, while 2-hydroxy ethyl acrylate (HEAc) was incorporated to the increase sieve size. UV/Vis measurement was used for determination of size as well as polydispersity of nanoparticles. They also investigated the effect of concentration of CdS and Ag NPs on the properties of the hybrid microgels by UV/Vis

spectroscopy. It was observed that increase of concentration of CdS from 0.027 to 0.08 g caused the red shift of absorption peak from 430 to 500 nm as well as increase in absorbance of CdS NPs. The size of CdS NPs was estimated to be in range of 3.0–5.9 nm depending upon composition of hybrid microgels. CdS-P(NIPAM-AA-HEAc) hybrid microgel samples were refluxed for 12 hours and analyzed by UV/Vis spectroscopy. Sharp absorption peaks with enhanced absorption were appeared in UV/Vis region after heating that controls the polydispersity of CdS NPs in microgels due to Ostwald ripening of small-sized nanoparticles. UV/Vis analysis of P(NIPAM-AA-HEAc) microgels fabricated with 0.23 and 0.39 g Ag NPs per gram of polymer microgels was also done. Broad adsorption peak at 411 nm was observed in case of hybrid microgels fabricated with 0.23 g Ag NPs/g polymer due to intrinsic size effect, while sharp peak with increased absorbance was observed in case of microgels fabricated with 0.39 g Ag NPs/g polymer that shows the increase in particle size with increase in concentration of Ag NPs in the dispersion.

Gorelikov et al. loaded Au NRs in P(NIPAM-AA) microgels and characterized this hybrid system using different techniques, including UV/Vis spectroscopy.<sup>[6]</sup> They noted that hybrid microgels dispersion has two peaks, one at 400 nm and another at 810 nm attributed to transverse and longitudinal SPR property of Au NRs loaded into the microgels, respectively. It means if some dispersion of hybrid system has two peaks in their spectra, it is an indication of presence of non-spherical/rod like nanoparticles loaded into the microgels. Lu and coworkers also confirmed the fabrication of Ag NPs in shell region of polystyrene-poly(N-isopropylacrylamide) [PST-p(NIPAM)] core-shell microgels by UV/Vis spectroscopy.<sup>[35]</sup> A single and narrow peak attributed to SPR of Ag NPs appeared at 410 nm in UV/Vis region indicates the successful loading of Ag NPs with spherical shape and narrow size distribution in polymer network.

Suzuki and coworkers prepared core-shell-shell microgels made of P(NIPAM) core surrounded by poly(N-isopropylacrylamide-(3-amino propyl methacrylamide hydrochloride)) [P(NIPAM-APMa)] shell having positively charged functional groups encapsulated in second shell made of P(NIPAM).<sup>[36]</sup> Au seeds were prepared in positively charged shell of core-shell-shell microgel particles by chemical reduction method. Then, Au NPs growth was carried by electroless plating from Au seeds. UV/Vis spectra of core-shell-shell microgels fabricated with Au seeds and Au NPs was scanned to elucidate their optical properties. No peak was observed in Au seed impregnated core-shell-shell microgel particles although hybrid microgel dispersion turned light pink. These results showed that size of Au seeds was very small almost less than 4nm and were unable to show SPR phenomenon. Yet, via electroless plating, Au seeds were grown to Au NPs of required size instead of synthesizing new Au NPs and inherent peak of Au NPs was appeared at 520 nm. Sharp peak appeared at 520 nm in UV/Vis region indicates spherical Au NPs with narrow size distribution. Wu et al. prepared silver-poly(N-isopropylacrylamide-acrylic acid-acrylamide) [Ag-P(NIPAM-AA-AAm)] hybrid microgels at 22°C, 38°C, and 43°C and impregnated them with Au NPs by in-situ reduction method using gold salt. Ag-P(NIPAM-AA-AAm) hybrid microgels and bimetallic fabricated Au-Ag-P(NIPAM-AA-AAm) hybrid

microgels samples were characterized by UV/Vis spectroscopy. It was observed that SPR band appearing at 400 nm relevant to Ag NPs disappeared, while band relevant to Au NPs was appeared at 500 nm in all three samples in case of Au-Ag-P(NIPAM-AA-AAm) hybrid microgels. Other researchers have also investigated metal nanoparticles fabrication in microgel particles by UV/Vis spectroscopy.<sup>[37,38]</sup>

### Study of growth of nanoparticles in microgels using UV/Vis spectroscopy

The growth of Plasmonic nanoparticles inside the microgels can be investigated using UV/Vis spectroscopy. When Plasmonic nanoparticles grow in microgels, the surface Plasmon band is red shifted. Kim et al. synthesized P(NIPAM-AA) microgels for in-situ growth of Au NPs.<sup>[39]</sup> Growth of metal nanoparticles core in polymer shell can also be investigated by using UV/Vis spectroscopy. Contreras-Caceres et al. prepared core-shell microgels with Au NPs core using surfactant cetyl trimethyl ammonium bromide (CTAB) and constructed P(NIPAM) shell around the Au NPs core by precipitation polymerization method.<sup>[40]</sup> They studied the influence of concentration of CTAB on morphology of Au NPs core by changing it from 0.015 to 0.05 M. UV spectra of two types of hybrid microgels indicated different morphology of central Au NPs core. By using 0.05 M CTAB, spherical shaped Au NP core was prepared while using 0.015 M solution of CTAB, flower like morphology (growth of random branches from central core in different directions) was observed. SPR band for spherical Au NPs core and flower like Au NPs core encapsulated P(NIPAM) core-shell hybrid microgels was red shifted from 571 to 589 and 669 to 687 nm, respectively, with increase in temperature of the medium from 15 to 50°C as well as SPR peaks were broaden. Red shift was more dominant in flower like Au NPs core encapsulated P(NIPAM) core-shell hybrid microgels with appearance of another band at 530 nm. Two bands were observed in flower like Au NPs core encapsulated core-shell microgels because two Plasmon modes were observed for Au nano star morphology.

Zhang et al. prepared P(NIPAM-AA-HEAc) microgels by precipitation polymerization and fabricated with Ag NPs using AgNO<sub>3</sub> salt as precursor of Ag<sup>+</sup> ions by UV irradiation at 365 nm.<sup>[41]</sup> Effect of irradiation time on growth of Ag NPs inside the polymer network was investigated by UV/Vis spectroscopy. It was observed that with increase of irradiation time, microgels dispersion was turned light pink to purple and then dark red indicating the formation and growth of Ag NPs. Before irradiation when Ag<sup>+</sup> ions were loaded in microgels dispersion, no peak was observed in UV/Vis spectra of microgel particles in range of 300–700 nm. After 3 minutes of irradiation, a shoulder peak at 520 nm was observed. After 6 minutes of irradiation, a peak at 440 nm was observed due to Plasmonic resonance phenomenon of Ag NPs. Absorbance intensity of synthesized Ag NPs was significantly enhanced. Wu et al. studied the growth of Au NPs in poly(2-dimethylaminoethyl methacrylate-co-3-(trimethoxysilyl) propyl methacrylate) [P(MAEm-tMSPm)] microgels by UV/Vis spectroscopy.<sup>[42]</sup> For this purpose, 16 μL of 100 mgmL<sup>-1</sup> solution of HAuCl<sub>4</sub> was added in microgels suspension, heated at 70°C and spectra were scanned at 0, 5, 10, 15, 20, and 30 minutes. It was observed

that SPR band of Au NPs was appeared in 500–550 nm range after 5 minutes of progress of reaction and was blue shifted as reaction time was increased. Reduction of gold ions to Au NPs was completed in 30 minutes.

Wu et al. prepared Ag NPs fabricated in P(NIPAM-AA-AAM) hybrid microgels at 22°C, 38°C, and 43°C and studied their optical properties at pH 8.48 and 3.33, respectively.<sup>[43]</sup> (Optical properties were studied at both pH greater and smaller than  $pK_a$  of AA). The volume phase transition temperature (VPTT) of P(NIPAM-AA-AAM) microgels lies in range of 32–45°C depending upon the pH of the medium and feed contents of microgels. So, Ag NPs were fabricated by in-situ reduction method in microgels at fully swollen, partially shrunken, and collapsed state. UV/Vis spectra indicated that small clusters of Ag were also formed along with Ag NPs during synthesis of hybrid microgels at all temperatures. Different position as well as shape of Plasmonic band was attained at different values of temperature of the medium. At 22°C, due to swollen state of microgel particles, large Ag NPs with broad size distribution were obtained. While at 38°C, due to partially swollen microgel particles, small-sized Ag NPs with narrow size distribution were obtained. At 43°C, when microgel particles were fully collapsed, faint SPR band appeared that indicates the presence of small number of Ag NPs along with Ag clusters.

### Study of growth of polymeric network around Plasmonic nanoparticles

The growth of polymeric network around Plasmonic nanoparticles can be studied by UV/Vis spectroscopy. When thickness of polymeric shell increases then Plasmonic band is shifted to higher wavelength due to increase of refractive index of the medium around nanoparticles.<sup>[44]</sup>

Lopez and coworkers prepared Au spheres, Au decahedra and Au nanostars by layer by layer assembly using CTAB as supporting material for Au spheres and poly(vinyl pyrrolidone) [p(VP)] for Au decahedra and Au nanostars, respectively.<sup>[44]</sup> They used Au spheres, Au decahedra and Au stars as seeds for growth of P(NIPAM) shell around them and studied their optical properties as a function of temperature of the medium by changing refractive index around central Au cores. Average diameter of P(NIPAM) encapsulated Au spheres, Au decahedra, and Au nanostars was found to be 58, 96 and 115 nm, respectively. SPR band appeared at 540, 620 and 850 nm for gold sphere, decahedra, and nanostar encapsulated in P(NIPAM) shell in UV/Vis spectra. Analysis shows that position of SPR band depends upon the size of central gold core. Increase in size of Au core red shifts the SPR band in UV/Vis region with increase of intensity as well as width of bands.

Effect of growth of shell on longitudinal  $\lambda_{SPR}$  of Au NRs encapsulated by polystyrene sulfonate (PSTs) layer and silica shell was investigated by Pastoriza-Santos et al. using UV/Vis spectroscopy.<sup>[45]</sup> It was observed that thickness of polymer shell influences the optical properties of composite system. Increase of shell thickness of Au NRs–PSTs–silica composite system showed no effect on transverse Plasmon band but longitudinal Plasmon band was red shifted. Red shifting of longitudinal Plasmon band of Au NRs was due to increase of local refractive index around Au NRs due to increased thickness of shell

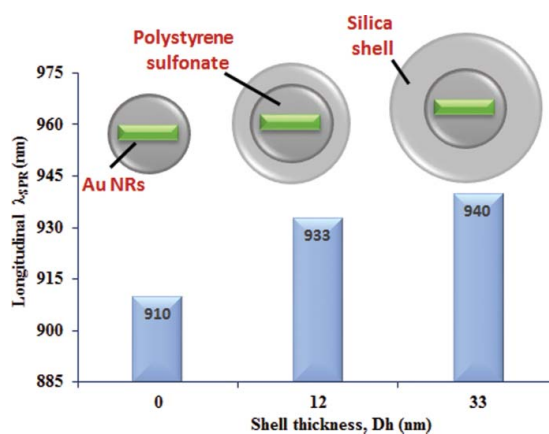


**Figure 1.** Effect of growth of shell thickness on longitudinal  $\lambda_{SPR}$  of Au NRs in Au NRs-PSTs-silica composite.<sup>[45]</sup>

region. It was observed that increase of shell thickness higher than 33 nm diameter did not affect the value of longitudinal  $\lambda_{SPR}$  of Au NRs as shown in Figure 1.

### Study of stability of metal nanoparticles in microgels by UV/Vis spectroscopy

Metal nanoparticles loaded into microgels have been found to be stable for long term due to donor–acceptor interaction between functional groups of polymeric network and metal nanoparticles as reported in literature.<sup>[46]</sup> The long-term stability of metal nanoparticles in microgels can be confirmed by using UV/Vis spectroscopy. Investigation of stability of NPs is based on measurement of SPR wavelength as a function of time of storage. For this purpose, dilute dispersion of hybrid microgels is stored in dark at room temperature and its UV/Vis spectra is scanned time to time and shift in  $\lambda_{SPR}$  value is noted. No shift in  $\lambda_{SPR}$  value with the passage of time indicates the stability of metal nanoparticles in polymeric network. We have recently reported the stability of Ag NPs loaded into poly(N-isopropylacrylamide-acrylamide) [P(NIPAM-AA)] microgels using UV/Vis spectroscopy.<sup>[47]</sup> For this purpose, dilute dispersion of P(NIPAM-AA) microgels was stored in a vial covered by aluminum foil and its UV/Vis spectra were scanned time to time up to 6 months after synthesis. No shift in  $\lambda_{SPR}$  value was noted which confirmed that Ag NPs are stable for long time for their practical applications. Khan et al. prepared Ag NPs by microwave irradiation method using  $AgNO_3$  salt as precursor of silver ions in P(NIPAM-AA) microgels template.<sup>[32]</sup> Ag NPs showed a peak in UV/Vis region at 429 nm due to SPR properties. They investigated the stability of Ag NPs in P(NIPAM-AA) microgel particles and observed that Ag NPs were stable even after 8 months of their preparation. Stability of Ag NPs was investigated by UV/Vis spectroscopy. No change in the value of  $\lambda_{SPR}$  was observed with slight decrease in absorbance intensity of peak at 429 nm. Also the color of Ag-P(NIPAM-AA) hybrid microgels sample remained the same. Results indicated the strong interaction between Ag NPs and microgels functional groups that prevented their aggregation and prolonged their life span. Wu and coworkers also investigated the stability of Ag-P(NIPAM-AA-AAM) hybrid microgels samples by UV/Vis spectrophotometry by scanning spectra of freshly

prepared samples and after passage of 1 month.<sup>[43]</sup> It was observed that Ag NPs were stabilized by microgels template for long time due to presence of amide and carboxylic acid chelating groups. UV/Vis spectra of silver-poly(N-isopropylacrylamide-(dimethylamino) ethyl methacrylate) [Ag-P(NIPAM-MAEm)] hybrid microgels showed that Ag NPs were highly stable inside the microgels sieves even after 8 months of synthesis. No change in catalytic activity of these hybrid systems was observed for reduction of methylene blue (MB) after 40 days of preparation as investigated by Tang and coworkers.<sup>[48]</sup>

### Study of stability of metal nanoparticles loaded microgels at different pH values

The pH of the medium is crucial for long-term storage of metal nanoparticles fabricated microgels. The hybrid polymer microgels have not been found to be stable in all values of pH of the medium. The pH range of medium in which hybrid microgels are stable depends upon the nature of functionalities of polymeric network. Farooqi et al. investigated the stability of Ag NPs fabricated in poly(N-isopropylacrylamide-methacrylic acid) [P(NIPAM-Ma)] microgels under acidic and basic conditions.<sup>[24]</sup> They stored Ag-P(NIPAM-Ma) hybrid microgels at pH 9.9 (high, basic) and 2.83 (low, acidic), separately while keeping all other conditions same. UV/Vis spectroscopy was used to investigate the stability of Ag NPs loaded microgels under above-mentioned pH values of the medium. UV spectra of Ag-P(NIPAM-Ma) hybrid microgels were scanned immediately after adjusting their pH and after 18 hours. It was observed that position and intensity of SPR band of Ag NPs was not changed at pH 9.9 even after passage of 18 hours. But in case of Ag-P(NIPAM-Ma) hybrid microgels at pH 2.83, SPR band appearing at 400 nm disappeared after keeping hybrid microgels at this pH for 18 hours. Actually, at high pH (9.9), carboxylic acid groups of Ma in P(NIPAM-Ma) microgels were in deprotonated form. These negatively charged groups induced large-scale swelling in polymer network as well as maintenance of stability of Ag NPs. While at low pH (2.83), carboxylate groups were protonated, polymer-polymer interaction was enhanced as a result, P(NIPAM-Ma) microgel particles were not only shrunked but microgel particles aggregated in acidic pH values as observed by different researchers.<sup>[24,49]</sup> Under such conditions, Ag NPs were also aggregated and their size was not remained in nano range due to shrinkage of microgel particles followed by aggregation. So, no peak appeared in UV/Vis region for Ag-P(NIPAM-Ma) hybrid microgels at pH 2.38. Ag NPs were stable for long time at pH > pK<sub>a</sub> of Ma in case of P(NIPAM-Ma) microgels, while they were highly unstable in acidic medium for that specific type of microgels.

### Study of optical properties of nanoparticles loaded in microgels

SPR wavelength ( $\lambda_{\text{SPR}}$ ) is a fascinating optical property of Plasmonic nanoparticles loaded into responsive polymer microgels and its value can be tuned by varying external stimuli like temperature<sup>[40]</sup> and pH<sup>[24]</sup> of the medium. The change in pH or temperature of the medium causes swelling or deswelling in microgel particles as a result of which variation in inter-nanoparticles distance and refractive index of the medium around nanoparticles

occurs. It causes change in the value of  $\lambda_{\text{SPR}}$ . UV/Vis spectroscopy can be used to study the tuning of optical properties of metal nanoparticles loaded into the microgels.

### Study of effect of pH of the medium on optical properties of metal nanoparticles

The pH value of the medium may affect the optical properties like  $\lambda_{\text{SPR}}$  of Plasmonic metal nanoparticles loaded into pH responsive microgel systems. Farooqi et al. reported the effect of pH of the medium on the value of  $\lambda_{\text{SPR}}$  of Ag NPs fabricated in P(NIPAM-Ma) microgels.<sup>[24]</sup> The value of  $\lambda_{\text{SPR}}$  was red shifted from 405 to 420 nm with increase of pH of the medium from 3.27 to 9.90. Intensity of SPR band was decreased with increase in pH of the medium. Value of  $\lambda_{\text{SPR}}$  of Ag NPs fabricated in P(NIPAM-Ma) microgels at different pH values of the medium is given in Table 1. The red shift in position of SPR band with an increase of the pH of the medium was due to deprotonation of Ma groups of P(NIPAM-Ma) microgel particles. Deprotonation of Ma groups caused swelling of microgel network. Due to swelling of microgel network, more water was rushed in polymer network. Distance between Ag NPs fabricated in microgel network was increased. As a result, electron density over the surface of Ag NPs was decreased as well as oscillation of electrons was also decreased. Slow oscillation of electron resonates with long wavelength electromagnetic radiation of UV/Vis region. Thus, SPR band of Ag NPs was appeared at longer wavelength. Thus, increase of pH of the medium red shifted the  $\lambda_{\text{SPR}}$  of Ag NPs fabricated in P(NIPAM-Ma) microgels. The increase in inter-nanoparticles distance could not be the only reason of red shift in their  $\lambda_{\text{SPR}}$  value. The studies must be carried out in reverse order in a reversible way to investigate that either shift is due to change in inter-nanoparticles distance or due to aggregation of some nanoparticles as a result of swelling of microgels. Moreover decrease of refractive index around Ag NPs loaded in P(NIPAM-Ma) microgels with increase in pH of the medium must be counted to investigate the actual cause of shift because different groups have reported different observations in this regard.

Many other researchers also investigated the pH tuned optical properties of hybrid microgels by UV/Vis spectroscopy.<sup>[48,50-52]</sup>

### Temperature tuned optical properties of microgels fabricated metal nanoparticles

The optical properties of metal nanoparticles fabricated in microgel particles can be tuned by varying the temperature of the medium. Temperature change induces swelling/shrinking in microgel network. As a result local refractive index around

**Table 1.** Effect of pH of the medium on  $\lambda_{\text{SPR}}$  of Ag NPs fabricated in P(NIPAM-Ma) microgels network.<sup>[24]</sup>

pH	$\lambda_{\text{SPR}}$ (nm)
3.27	405
6.08	410
8.38	415
8.97	418
9.90	420

metal nanoparticles is changed and reversible shift in SPR frequency occurs.<sup>[44]</sup>

Frenandez-Lopez et al. studied the effect of temperature on optical properties of Au NPs (spheres, decahedrons, and nano-stars) fabricated P(NIPAM) composite microgels by UV/Vis spectroscopy.<sup>[44]</sup> Temperature modulated optical properties of these three types of hybrid microgels consisting of morphologically different Au central cores were also investigated. Due to volume phase transition (VPT) of P(NIPAM) microgels, refractive index around Au cores was changed which tuned their optical properties. Data indicated that temperature tuned shifting of SPR band depends upon the morphology of central Au core. Slight change in position of SPR band of Au spheres and Au decahedron in response to change in temperature of the medium from 20 to 50°C was observed but large shift in SPR band was observed in case of Au nano star core due to presence of sharp tips in these particles. It was observed that SPR band was red shifted with increase of temperature of the medium from 22 to 44°C with slight increase in absorbance value at  $\lambda_{\text{SPR}}$  in all composite microgels. Values of  $\lambda_{\text{SPR}}$  and relevant absorbance of different Au particles fabricated hybrid microgels at two different values of temperature are given in Table 2. It was also observed that position of SPR band also depends upon the shape of metal nanoparticles. Temperature tuned reversible optical properties of gold nano spheres having diameter of 58 nm encapsulated in P(NIPAM) microgels was also investigated by UV/Vis spectroscopy at temperature of 20 and 40°C. It was observed that SPR band of hybrid microgels was appeared at 540 and 553 nm at temperature 20 and 40°C, respectively, even after six heating and cooling cycles.

Shah et al. investigated the optical properties of Ag-P(NIPAM-AAm-VAc) hybrid microgels as a function of temperature of the medium at pH 8.54 and 2.84.<sup>[53]</sup> They observed

that temperature has no influence on SPR band at pH 8.54 due to swelling state of microgels and presence of equally distributed Ag NPs. However, at pH 2.84,  $\lambda_{\text{SPR}}$  was red shifted from 409 to 419 nm with increase in temperature of the medium from 20 to 40°C. Absorbance value of SPR band was also increased with increase in temperature of the medium.







Suzuki et al. also investigated the temperature tuned optical properties of Au NPs impregnated poly(N-isopropylacrylamide-glycidylmethacrylate) [Ag-P(NIPMA-GMa)] hybrid microgel particles and observed the red shift in SPR band with increase in temperature of the medium.<sup>[54]</sup> Dong and coworkers investigated that  $\lambda_{\text{SPR}}$  of Ag NPs fabricated in P(NIPAM-AA) microgels was shifted from 402 to 417 nm with increase of temperature of the medium from 25 to 45°C, while absorbance value of SPR band was decreased.<sup>[46]</sup> They also evaluated the temperature tuned reversible behavior of Ag-P(NIPAM-AA) hybrid microgels by UV/Vis spectroscopy in temperature range of 25–45°C in aqueous medium. Many other researchers have investigated temperature-dependent optical properties of metal nanoparticles fabricated hybrid microgels by UV/Vis spectroscopy.<sup>[55–56]</sup>

### Study of feed content of cross-linker on size of metal nanoparticles

Concentration of cross-linker used during the synthesis of microgel particles controls their sieve size and alternatively the size as well as optical properties of metal nanoparticles fabricated in these sieves.

Farooqi et al. prepared Ag NPs fabricated Ag-P(NIPAM-AA) hybrid microgel particles with 2, 4, 6, and 8 mol% MBiS.<sup>[5]</sup> They investigated the optical properties of Ag NPs fabricated in P(NIPAM-AA) microgels samples as a function of feed contents

**Table 2.** Effect of temperature of the medium on optical properties of P(NIPAM) hybrid microgels fabricated with different shaped Au particles.<sup>[44]</sup>

Composite microgels	Temperature = 22°C			Temperature = 44°C		
	$\lambda_{\text{SPR}}$ (nm)	Absorbance (a.u)	Pictorial diagram	$\lambda_{\text{SPR}}$ (nm)	Absorbance (a.u)	Pictorial diagram
Au spheres-P(NIPAM)	540	0.95		555	1.01	
Au decahedra-P(NIPAM)	616	0.97		633	1.02	
Au nanostar-P(NIPAM)	826	0.97		858	1.03	

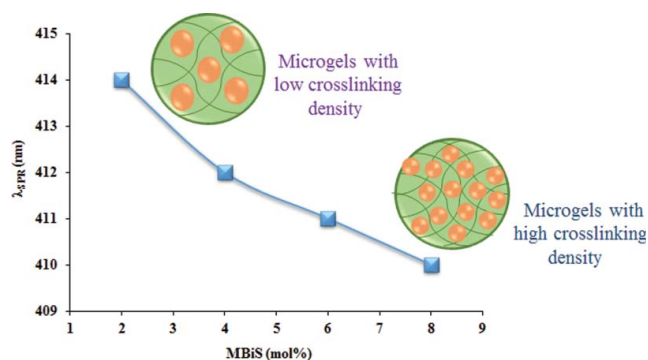


**Figure 2.** Effect of feed contents of cross-linker (MBiS) on  $\lambda_{SPR}$  of Ag NPs fabricated in P(NIPAM-AA) microgels made of different mole% of MBiS.<sup>[51]</sup>

of cross-linker by UV/Vis spectroscopy. Effect of concentration of MBiS on  $\lambda_{SPR}$  value of Ag NPs fabricated in P(NIPAM-AA) microgels at pH 9.88 and temperature 28°C is shown in Figure 2. Size of Ag NPs was decreased with increase of feed concentration of MBiS as shown in Figure 2 due to increase in cross-linking density of P(NIPAM-AA) microgels. Decreased size of Ag NPs induced blue shift in  $\lambda_{SPR}$  of Ag NPs as investigated by UV/Vis spectroscopy. Contreras-caceres et al. also investigated the influence of content of cross-linker on size of Au NPs encapsulated P(NIPAM) core-shell hybrid microgels.<sup>[21]</sup>  $\lambda_{SPR}$  of Au NPs was found to be blue shifted with increase of feed content of MBiS cross-linker.

#### Study of effect of feed content of ionic co-monomer on size of metal nanoparticles

Concentration of ionic co-monomer used during synthesis of microgel particles controls their sieve size and ultimately the size and optical properties of metal nanoparticles fabricated in them. Farooqi and coworkers prepared P(NIPAM-AA) microgels consist of 1, 3, 5, and 7 mol% AA contents and used these microgel samples as micro-reactor for preparation of Ag NPs.<sup>[57]</sup> They scanned the UV/Vis spectra of all four types of hybrid microgel samples to evaluate the value of  $\lambda_{SPR}$  and relative absorbance of Ag NPs fabricated in P(NIPAM-AA) microgels at pH 10.37 and temperature 18 °C. The relation between mol% of AA and the value of  $\lambda_{SPR}$  as well as relative absorbance is shown in Figure 3. It was observed that the value of  $\lambda_{SPR}$  of Ag NPs fabricated in microgels network was increased with increase of concentration of AA. Appearance of single peak in all spectra in UV/Vis region shows that Ag NPs were spherical in shape. All peaks appearing in UV/Vis region for all hybrid microgels samples were different in positions ( $\lambda_{SPR}$ ) and broadness which showed that Ag NPs were different in their number, size and size distribution. As shown in Figure 3, value of  $\lambda_{SPR}$  was changed from 409 to 430 nm with increase of feed concentration of AA from 1 to 7 mol%. It means high concentration of AA leads to increase in number of carboxylic acid (COOH) groups in network which ultimately enhances the concentration of silver ions in the network. Size of Ag NPs increases with increase of AA content due to reduction of high number of silver ions contents in the sieves of microgels. Thus, red shift in  $\lambda_{SPR}$  value along with increase in absorbance at  $\lambda_{SPR}$  was observed with increase of feed concentration of AA. These

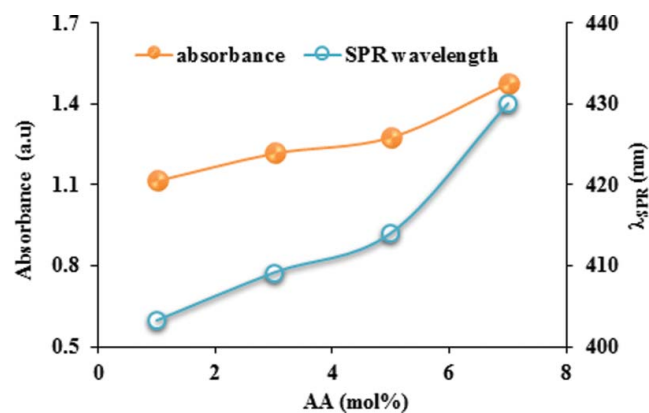


**Figure 3.** Effect of feed contents of acrylic acid on value of  $\lambda_{SPR}$  as well as absorbance of Ag NPs fabricated in P(NIPAM-AA) microgels having different feed concentration of AA.<sup>[57]</sup>

results show increased number of Ag NPs having large size with increase of AA contents of microgels from 1 to 7 mol%. These carboxylic acid groups are deprotonated at pH >  $pK_a$  of AA and ultimately more silver ions are attracted inside the microgel sieves which results in synthesis of large number of particles with large size.

#### Effect of feed content of precursor salt on size and shape of metal nanoparticles fabricated in microgels

Concentration of salt used to fabricate metal nanoparticles in polymeric network also plays a critical role in the size and shape control. Suzuki and coworkers prepared poly(glycidyl methacrylate-N-isopropylacrylamide) core encapsulated in P(NIPAM) shell and fabricated these P(GMa-NIPAM)-P(NIPAM) core-shell microgels with Au NPs and then electroless gold plates.<sup>[58]</sup> Electroless Au plated P(GMa-NIPAM)-P(NIPAM) core-shell hybrid microgel particles fabricated with different amount of gold salt for synthesis of gold plates were characterized by UV/Vis spectroscopy. Relation between volume of HAuCl<sub>4</sub> salt used for synthesis of electroless plated core-shell hybrid microgel particles and  $\lambda_{SPR}$  of fabricated Au NPs is shown in Figure 4. A weak absorption peak was appeared at 532 nm in P(GMa-NIPAM)-P(NIPAM) core-shell microgels fabricated with low amount of gold salt and as a result small-sized Au NPs were formed. This peak was red shifted with slight increase in absorbance intensity as amount of gold salt was increased. This shows increase in size of Au NPs with increase of concentration of precursor salt. Diameter of Au NPs was increased from 10 to 15 nm with increase of volume of gold salt from 10 to 50  $\mu$ L and SPR band was red shifted from 532 to 555 nm. Peaks were become more broaden and shifted to longer wavelength with increase of used quantity of Au NPs precursor salt.

#### Effect of feed content of carbohydrate polymers on optical properties of metal nanoparticles fabricated in microgels

Vimala and coworkers prepared interpenetrating hydrogel network made up of poly(acrylamide) [P(AAM)] integrated with three different carbohydrate polymers like carboxymethylcellulose



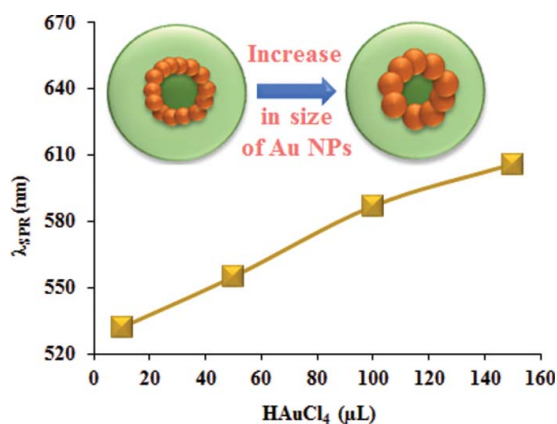


**Figure 4.** Effect of feed concentration of gold salt on  $\lambda_{SPR}$  of Au nanoshells impregnated in core-shell boundary of P(GMA-NIPAM)-P(NIPAM) core-shell microgels.<sup>[58]</sup>

(CMc), starch (SRt) and gum acacia (Ga).<sup>[59]</sup> Concentration of all three carbohydrate polymers was changed from 0.1 to 0.5 g during synthesis of interpenetrating network and these hydrogel samples were used as micro-reactor for fabrication of Ag NPs. Ag NPs fabricated P(Am)-CMc, P(AAm)-SRt and P(AAm)-Ga composite hydrogels consisting of different feed contents of carbohydrate polymer were analyzed by UV/Vis spectroscopy. It was observed that different groups present in composite hydrogels like COOH, OH, NH<sub>2</sub>, and CONH acted as coordinating agents to stabilize Ag NPs inside the interpenetrating network. UV/Vis analysis showed increase of absorbance of peak at 416 nm and at 408–416 nm in Ag-P(Am)-Ga and Ag-P(AAm)-CMc composite hydrogels, respectively, with increase of concentration of Ga and carboxy methylcellulose (CMc) due to increase of size of fabricated Ag NPs. Actually, high concentration of carbohydrate polymers induced large number of functional groups inside hydrogel network. As a result, large numbers of silver ions were fabricated in hydrogel network that leads to large-sized Ag NPs. In case of Ag-P(AAm)-SRt composite microgels, random increase/decrease in absorbance of peak at 416 nm was observed with increase feed content of SRt from 0.1 to 0.5 g. This randomness in behavior may be due to solubility of starch content in aqueous medium. Thus, UV/Vis study speculates that CMc and Ga incorporated composite hydrogels provide enough space for fabrication of large number of Ag NPs as compared to SRt impregnated composite hydrogels.

### Study of tuning of aspect ratio of plasmonic nanomaterials loaded into microgels

High aspect ratio nanomaterial has gained significant attention recently due to its potential applications in various areas. Many reports are available in literature on loading of high aspect ratio nanoparticles in responsive microgels.<sup>[60–64]</sup> Metal NRs show different optical properties as compared to spherical metal nanoparticles due to their shape. Au NRs impregnated microgels absorb light of NIR. It is well known that in this region, minimum light absorption by body tissue like hemoglobin occurs. Thus, near IR light can penetrate deep inside the body for treatment purpose without causing any damage in the body. Au NRs may have longitudinal surface Plasmon band in near IR region depending upon their aspect ratios. Irradiation of Au NRs by near IR

radiation induces photothermal effect in hybrid system. As a result, microgel particles loaded with Au NR undergo VPT due to heating caused by conversion of light energy into heat energy as a result of irradiation process and find applications in sensing and drug delivery.<sup>[64]</sup>

Kawano and coworkers prepared Au NRs having aspect ratio 5.7 and encapsulated them in P(NIPAM) microgel shell by precipitation polymerization.<sup>[64]</sup> Au NRs-P(NIPAM) composite microgels were analyzed by UV/Vis spectroscopy. Longitudinal SPR band of Au NRs fabricated in P(NIPAM) microgels were found in NIR range by Rodriguez-Fernandez and coworkers using UV/Vis spectroscopy.<sup>[63]</sup> It was observed that VPT of P(NIPAM) microgels can be monitored due to high sensitivity of longitudinal Plasmon band of Au NRs to local refractive index of polymer network. Longitudinal Plasmon band of Au NRs was shifted from 828 to 862 nm with increase of temperature of the medium from 16 to 60 °C. Actually, refractive index of P(NIPAM) microgel increases due to its collapsed state under the high temperature (60 °C). High absorption at longitudinal Plasmon resonance indicates that the Au NRs can be used as excellent candidate for NIR photothermal heat source.

Das et al. impregnated Au NRs in poly(N-isopropylacrylamide-maleic acid) [P(NIPAM-Mac)] microgels and characterize these composite systems by UV/Vis spectroscopy.<sup>[31]</sup> They investigated that these Au NRs impregnated hybrid microgels show remarkable absorption in NIR and can be used as photo thermally controlled drug delivery vehicles. Gorelikov et al. fabricated Au NRs with different aspect ratios using seed mediated growth method.<sup>[6]</sup> The increase in length of NRs with variation of reagents was investigated by UV/Vis spectroscopy. Change in the value of  $\lambda_{SPR}$  of Au NRs fabricated in P(NIPAM-AA) microgels with change of aspect ratio as well as light irradiated shrinkage of microgel network and release of drug is shown in Figure 5.

Au NRs-P(NIPAM-AA) hybrid microgels absorb light energy of NIR and convert it in to heat energy. This heat energy induces VPT in P(NIPAM-AA) microgels. Due to the shrinkage of microgel particles, loaded drug can be released at controlled rate to the targeted site.

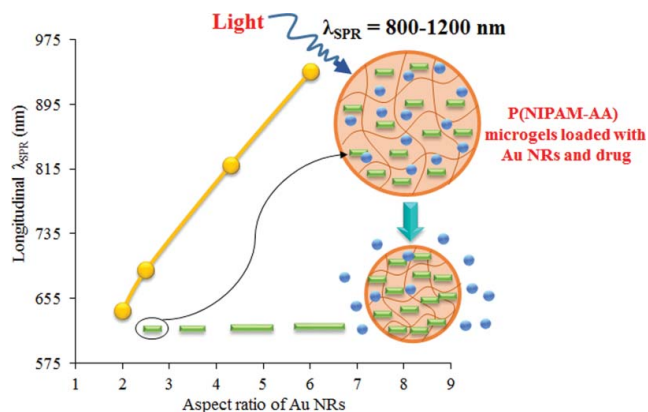


**Figure 5.** Relation between aspect ratio and longitudinal  $\lambda_{SPR}$  of Au NRs impregnated in P(NIPAM-AA) microgels along with release of drug from shrank microgel network due to near infrared irradiation.<sup>[6]</sup>

## Study of properties of pure and hybrid microgels by UV/Vis spectroscopy

The UV/Vis spectroscopy cannot only be used for investigation of properties of hybrid microgels due to their inorganic component but it can also be used for determination of characteristics of hybrid microgels that are only due to responsive polymeric network. For example, NIPAM-based polymer microgels are well-known thermo-responsive polymer microgels. They show sudden decrease in their size at particular temperature which is known as VPTT. The value of VPTT of P(NIPAM) microgels in aqueous medium is found to be 32°C. The UV/Vis spectroscopy has been reported as a tool for determination of VPTT of NIPAM-based microgels. Khan et al. used UV/Vis spectroscopy for determination of VPTT of P(NIPAM-AA) microgels in aqueous medium.<sup>[65]</sup> They used cloud point method (turbidity method) for determination of VPTT of P(NIPAM-AA) microgels and measured the values of percentage transmittance of colloidal dispersion of P(NIPAM-AA) microgels as a function of temperature using UV/Vis spectrophotometry. They plotted percentage transmittance versus temperature of microgels dispersion and noted that the value of percentage transmittance significantly dropped at VPTT due to the increase in turbidity of colloidal system. They also measured the value of VPTT of the microgels using DLS and compared it to the value of VPTT of microgels dispersion measured by UV/Vis spectrophotometry under the same conditions. The values of VPTT measured by UV/Vis spectroscopy was found to be exactly same as that measured by DLS. They investigated the effect of AA contents and pH of the medium on the value of VPTT in aqueous medium using same technique. Wang et al. used measurement of percentage transmittance as a function of temperature for determination of VPTT of poly(N-isopropylacrylamide-co-4-vinylpyridine) [PNIPAM-P4VP] microgels.<sup>[66]</sup>


Wang et al. used absorbance measurements of dispersion of P(NIPAM-AAm) microgels at 500 nm for determination of their VPTT in aqueous medium.<sup>[27]</sup> The VPTT of microgels

measured by UV/Vis spectroscopy was found to be exactly same as that measured by the DLS. They reported that the DLS is a good technique for determination of VPTT of microgels but it cannot be used to study the kinetics of swelling/deswelling of microgel particles. However, kinetics of phase transition of P(NIPAM-AAm) microgels can be studied by measuring the transmittance of dispersion (30 mg/mL<sup>-1</sup>) as a function of time at VPTT of the microgels with mole ratio of NIPAM to AAm 100:0, 95:5, 90:10, and 85:15. They studied the effect of AAm content in microgels and the concentration of microgels on time required for equilibrium swelling and deswelling using UV/Vis spectroscopy. They reported that UV/Vis spectroscopy is an excellent tool for study of kinetics of swelling and deswelling of microgels with small particle size.

Contreras-Caceres et al. used UV/Vis spectroscopy for determination of VPTT of Au-P(NIPAM) hybrid microgels with Au NPs core and P(NIPAM) shell by measuring the change in the values of both absorbance and SPR wavelength ( $\lambda_{\text{SPR}}$ ) as a function of temperature of the medium.<sup>[40]</sup> The value of absorbance of Au-P(NIPAM) core-shell microgels at 400 nm and position of SPR band as function of temperature of the medium is given in Table 3. Actually, volume of P(NIPAM) shell was decreased with change of temperature of the medium from 10 to 50 °C, which ultimately tuned the position of SPR band of Au NPs core due to modification of refractive index around them. SPR band was red shifted with increase of absorbance as temperature of the medium was changed from 10 to 50 °C. As temperature increases, microgel particles shrink and their refractive index increases that results in increase of Rayleigh scattering. Local refractive index around Au NPs core also increases, which results in red shift of SPR band as shown in Table 3. Absorbance of SPR band at low wavelength (400 nm) was increased that shows increased turbidity of Au-P(NIPAM) core-shell microgels with increase of temperature of the medium. Results showed that curve obtained between temperature of medium and position of SPR band as well as absorbance resemble the curve

**Table 3.** Effect of temperature on position of SPR band and absorbance (at 400 nm) of Au NPs core of Au-P(NIPAM) core-shell hybrid microgels.<sup>[37]</sup>

Temperature (°C)	$\lambda_{\text{SPR}}$ (nm)	Absorbance (a.u)
10	544	0.233
20	545	0.238
30	548	0.251
40	553	0.300
50	555	0.327



obtained by DLS analysis to study temperature responsive behavior of microgel particles. Thus, UV/Vis spectra obtained between temperature of the medium and position of SPR band as well as absorbance can be used to find VPTT of the microgel and hybrid microgel particles. Thus, absorbance measurement as function of temperature can be used for determination of VPTT of both pure and hybrid microgels but the method based on measurement of  $\lambda_{\text{SPR}}$  as a function of temperature can only be used for determination of VPTT of hybrid microgels.

Many other researchers have reported VPTT of different microgel suspensions by UV/Vis spectroscopy.<sup>[67,68]</sup>

## Study of catalysis in the presence of hybrid microgels

### Monitoring of catalytic reaction

UV/Vis spectroscopy is an excellent tool to investigate the catalytic activity of hybrid microgels toward a model reaction. Reduction of 4-Np is generally used as a model reaction for investigation of catalytic activity of metal nanoparticles loaded into microgels.<sup>[26,42,55,56]</sup> Catalytic reduction of other nitroaromatic compounds, like 2-nitrophenol (2-Np)<sup>[69]</sup> nitrobenzene (Nb),<sup>[30,70]</sup> 2-nitroaniline (2-NA),<sup>[24]</sup> 4-nitroaniline (4-NA)<sup>[19]</sup>, as well as dyes like Eryosin Y (EY),<sup>[69]</sup> methylene blue (MB)<sup>[56]</sup>, Congo red (CR)<sup>[71]</sup>, and methyl orange (MO)<sup>[69]</sup> have also been monitored by UV/Vis spectroscopy. The progress of reduction of 4-Np is investigated using UV/Vis spectrophotometry because 4-Np and corresponding product 4-AP absorbs at 400 nm and 300 nm, respectively. Catalytic reduction of 4-Np is carried out in the presence of hybrid microgels using sodium borohydride as reducing agent in quartz cell and reduction spectra is scanned in the wavelength range of 200–600 nm. The value of absorbance at 400 nm decreases with time due to consumption of 4-Np while that at 300 nm increases with increase in time due to formation of 4-AP. Catalytic activity of a lot of hybrid microgels toward the catalytic reduction of 4-Np has been investigated using UV/Vis spectrophotometry.<sup>[5,35,47,57,72–74]</sup> For example, Lu et al. used UV/Vis spectrophotometry for monitoring of catalytic reduction of 4-NP using Ag NPs impregnated Ag-PST-P(NIPAM) core-shell hybrid microgels system as catalyst in aqueous medium.<sup>[35]</sup> Begum et al. investigated the catalytic reduction of 4-Np using sodium borohydride reducing agent in the presence of Ag-P(NIPAM-AAm) hybrid microgels by UV/Vis spectroscopy.<sup>[47]</sup> It was observed that 4-Np showed peak at 300 nm in UV/Vis region. This peak was shifted to 400 nm in the presence of sodium borohydride due to conversion of 4-Np to 4-nitrophenolate ion. In presence of Ag-P(NIPAM-AAm) hybrid microgels catalyst, absorbance of peak at 400 nm was decreased due to decrease in concentration of 4-Np, while new peak was appeared at 300 nm due to formation of 4-AP. Reduction of 0.061 mM 4-Np was completed in 25 minutes using 9.15 mM NaBH<sub>4</sub> and 23.90 mgmL<sup>-1</sup> hybrid microgels catalyst at 32 °C temperature. Pich and coworkers reported the use of Au NPs fabricated poly(N-vinylcaprolactam-acetoacetoxyethyl methacrylate) [(P(VC-AAma))] hybrid microgels catalyst for reduction of 4-nitrophenol.<sup>[73]</sup> Au NPs fabricated in microgel network showed high catalytic activity as compared to naked Au NPs having similar properties for reduction of 4-nitrophenol. Many

other researchers reported the monitoring of various reactions catalyzed by hybrid microgels catalyst using UV/Vis spectrophotometry.<sup>[25,30,70, 71,75–77]</sup>

### Determination of rate constant

The UV/Vis spectroscopy is widely used to determine the value of apparent rate constant ( $k_{\text{app}}$ ) for catalytic reaction occurring in the presence of hybrid microgels.<sup>[5,12,19,24,25,47,57,72,75,78]</sup> For example, the determination of the value of  $k_{\text{app}}$  for catalytic reduction of 4-Np in the presence of various temperature responsive hybrid microgels has been reported recently by us and others.<sup>[20,47,53,62,79]</sup> For determination of  $k_{\text{app}}$  for catalytic reduction of 4-Np,  $\ln(A_t/A_o)$  is plotted as a function of time using following equations.

$$\ln\left(\frac{C_t}{C_o}\right) = -k_{\text{app}}t \quad (1)$$

$$\ln\left(\frac{A_t}{A_o}\right) = -k_{\text{app}}t \quad (2)$$

where  $A_t$  is the absorbance of 4-Np at any time, while  $A_o$  is the value of absorbance at zero time. Pich et al. determined the value of  $k_{\text{app}}$  for reduction of 4-Np using Au-P(VC-AAEm) hybrid microgels catalyst by UV/Vis spectrophotometry.<sup>[73]</sup> They observed that the induction time was shortened with the increase of catalyst dose. Induction time is the time period in which reaction does not start even after addition of catalyst in reaction mixture and has been observed in catalysis by hybrid microgels.<sup>[24]</sup> Absorbance of 4-Np was measured at 400 nm at different time intervals during progress of reaction. The value of  $k_{\text{app}}$  was determined from linear part of the graph plotted between  $\ln(A_t/A_o)$  and time. It was observed that the value of  $\ln(A_t/A_o)$  was decreased with increase of reaction time. Value of  $k_{\text{app}}$  was increased from  $1.07 \times 10^{-3}$  to  $3.96 \times 10^{-3} \text{ s}^{-1}$  with increase of catalyst dose from  $4.85 \times 10^{-6}$  to  $2.10 \times 10^{-5} \text{ gL}^{-1}$ , respectively. They also studied the effect of Au NPs contents on the value of  $k_{\text{app}}$  for reduction of 4-nitrophenol. The value of  $k_{\text{app}}$  was increased from  $1.07 \times 10^{-3}$  to  $3.69 \times 10^{-3} \text{ s}^{-1}$  with increase of Au NPs contents from 5.1 to 10.3 wt%, respectively. The effect of temperature on the value of  $k_{\text{app}}$  for reduction of 4-Np using Au-P(VC-AAEm) hybrid microgels and naked Au NPs catalyst was also investigated by changing temperature from 10 to 40 °C. The value of  $k_{\text{app}}$  was increased with the increase of temperature of the medium but high catalytic efficiency was observed in case of hybrid microgels catalyst as compared to naked Au NPs. Many other researchers have also determined the value of  $k_{\text{app}}$  for catalytic reduction of various compounds using UV/Vis spectroscopy.<sup>[25,66,75]</sup>

### Effect of different factors on value of $k_{\text{app}}$

Effect of different factors like concentration of catalyst,<sup>[48,80]</sup> reducing agent,<sup>[69,70]</sup> substrate being reduced, temperature,<sup>[48,72]</sup> and pH of the medium<sup>[19]</sup> on the value of  $k_{\text{app}}$  has also been studied by UV/Vis spectroscopy. Temperature of the medium tunes the catalytic activity of hybrid microgels for various

organic reactions. Lu et al. investigated the influence of temperature of the medium on rate of reduction of 4-Np using Ag-PST-P (NIPAM) core-shell hybrid microgels as catalyst by changing its value from 10 to 40 °C.<sup>[35]</sup> Temperature dependence of apparent rate constant for reduction of 4-Np deviates from Arrhenius behavior due to temperature induced VPT of PST-P(NIPAM) core-shell microgel particles. At low temperature (from 10 to 25 °C), when hybrid microgels shell was swollen and reactants were easily diffused into shell region, relation between temperature and apparent rate constant for reduction of 4-Np was Arrhenius type. Further increase of temperature >25 °C induced shrinkage of microgels shell. Due to shrinkage of shell, sieves size was decreased as water was expelled out and diffusion of reactants to approach Ag NPs surface was decreased. As a result, rate of reduction of 4-Np was decreased and significant decrease in the value of apparent rate constant ( $k_{app}$ ) was noted. Thus, in this region, increase of  $k_{app}$  with increase of temperature of the medium was overcome by reactants diffusion barrier. The  $k_{app}$  value approaches to its minimum value at VPTT of core-shell hybrid microgels. After VPT of microgels shell, network density is increased to maximum level. Further increase in temperature causes increase in the value of  $k_{app}$  and as a result rate of reduction of 4-Np increases. Many other researchers have studied the influence of temperature of the medium on catalytic reduction of various organic compounds by UV/Vis spectroscopy and found the same results.<sup>[79]</sup>

### Determination of Arrhenius and Eyring parameters

The value of apparent rate constant ( $k_{app}$ ) can be measured at different temperature using UV/Vis spectrophotometry. The natural logarithm of the value of apparent rate constant is plotted against inverse of temperature for determination of Arrhenius parameters like activation energy ( $E_a$ ) and pre-exponential factor (A) according to following equation.<sup>[48]</sup>

$$\ln k_{app} = -\frac{E_a}{R} \frac{1}{T} + \ln A \quad (3)$$

The value of activation energy and pre-exponential factor is determined from the slope and intercept of the plot of natural logarithm of the value of  $k_{app}$  versus  $1/T$ , respectively. Tang et al. study the influence of temperature on reduction of MB in the presence of Ag NPs impregnated P(NIPAM-MAEm) hybrid microgels catalyst using UV/Vis spectroscopy and calculated the Arrhenius parameters.<sup>[48]</sup> The value of  $E_a$  for reduction of MB was found to be 62.0 kJmol<sup>-1</sup>. Linear relation between  $\ln k_{app}$  and  $1/T$  also indicates that reduction of MB followed Arrhenius equation. They also calculated activation enthalpy ( $\Delta H^\ddagger$ ) and activation entropy ( $\Delta S^\ddagger$ ) from slope and intercept of Eyring plot, respectively using the following equation:

$$\ln\left(\frac{k_{app}}{T}\right) = -\frac{\Delta H^\ddagger}{R} \left(\frac{1}{T}\right) + \ln\left(\frac{k_B}{h}\right) + \frac{\Delta S^\ddagger}{R} \quad (4)$$

Values of  $\Delta H^\ddagger$  and  $\Delta S^\ddagger$  were found to be 59.5 kJmol<sup>-1</sup> and -68.8 Jmol<sup>-1</sup>K<sup>-1</sup>, respectively. Pich et al. determined the value of activation energy ( $E_a$ ) for reduction of 4-Np using Au-P

(VC-AAEm) hybrid microgel and naked Au NPs catalyst.<sup>[74]</sup> The value of  $E_a$  was found to be 36 and 71 kJmol<sup>-1</sup> for hybrid microgels and naked Au NPs catalyst, respectively. Results indicated unique catalytic properties of hybrid microgels as compared to naked Au NPs. Naseer and coworkers reported the use of Co-P(AA-AAm) and Cu-P(AA-AAm) hybrid microgels catalyst for reduction of 4-Np at different values of temperature of the medium.<sup>[18]</sup> Both type of composite catalysts were found to be as efficient catalysts for reduction of 4-Np. Activation energy ( $E_a$ ) calculated by using Arrhenius equation for the reduction of 4-Np was found to be 17.083 and 87.87 kJmol<sup>-1</sup> for Co-P (Ac-Am) and Cu-P(Ac-AAm) hybrid microgels, respectively. Value of activation enthalpy and activation entropy for reduction of 4-Np was calculated by using Eyring equation (equation 4). Value of  $\Delta H^\ddagger$  and  $\Delta S^\ddagger$  were found to be 278.48 Jmol<sup>-1</sup> and -196.65 Jmol<sup>-1</sup>K<sup>-1</sup>, respectively, for reduction of 4-Np using Cu-P(Ac-AAm) hybrid microgels as catalyst. The value of  $\Delta G^\ddagger$  was calculated by using the following equation:

$$\Delta G^\ddagger = \Delta H^\ddagger - T\Delta S^\ddagger \quad (5)$$

Ajmal et al. also calculated the activation energy for reduction of 4-Np using Ag-P(NIPAM-Ma-AAm) hybrid microgels catalyst.<sup>[51]</sup> Value of activation energy was decreased from 33.28 to 26.56 kJmol<sup>-1</sup> with increase of catalyst dose from 0.02 to 0.06 mL, respectively. Many other researchers have calculated the value of Arrhenius and Eyring parameters for reduction reaction catalyzed by hybrid microgels using UV/Vis spectroscopy.<sup>[81]</sup>

### Summary and future prospective

The UV/Vis spectroscopy is a simple and easily available technique for study of some important fundamental properties of pure and hybrid microgels. UV/Vis spectroscopy alone is not a sufficient technique to completely characterize the hybrid microgel system but it may be a very useful technique to extract some necessary information along with other characterization techniques. The value of VPTT of thermo-sensitive pure microgels can be determined using turbidity method from the plot of percentage transmittance versus temperature. The measurement of  $\lambda_{SPR}$  using UV/Vis spectrophotometer at different temperature may be a useful tool for determination of VPTT of hybrid microgels but it has been rarely reported in literature. The stability of Plasmonic nanoparticles loaded into microgels can be investigated by measuring their  $\lambda_{SPR}$  values at different times of storage. Only a few reports are available on measurement of transmittance of microgels dispersion for investigation of kinetics of swelling and deswelling of microgels and hybrid microgels. Time-dependent swelling and deswelling kinetics of various microgels should be investigated in detail using UV/Vis spectroscopy. Time required for equilibrium swelling and deswelling is an important parameter for their practical applications. UV/Vis spectroscopy is an excellent tool for this purpose. The study of VPT of smart polymer microgels having Plasmonic nanoparticles by measurement of  $\lambda_{SPR}$  has been rarely reported in literature. Determination of VPTT of hybrid microgels based on  $\lambda_{SPR}$  measurement may be reported in future.

## Abbreviations

AA	Acrylic acid
AAM	Acrylamide
AAMa	Acetoacetoxyethyl methacrylate
AFM	Atomic force microscopy
APMa	N-(3-aminopropyl) methacrylamide hydrochloride
Au NPs	Gold nanoparticles
Au NRs	Gold nanorods
Ag NPs	Silver nanoparticles
CdS	Cadmium sulfide
CMC	Carboxy methylcellulose
CR	Congo red
CTAB	Cetyltrimethyl ammonium bromide
DLS	Dynamic light scattering
EY	Eyosin Y
FTIR	Fourier transform infrared
Ga	Gum acacia
GMa	Glycidyl methacrylate
HEa	Hydroxy ethylacrylate
LCST	Lowest critical solution temperature
Ma	Methacrylic acid
Mac	Maleic acid
MAEm	(dimethyl amino) ethyl methacrylate
MB	Methylene blue
MBiS	N,N-methylene bis acrylamide
MO	Methyl orange
Nac	Sodium acrylate
NaBH <sub>4</sub>	Sodium borohydride
Nb	Nitrobenzene 4
NIPAM	N-isopropylacrylamide
Np	4-nitrophenol
NRs	Nanorods
PSTs	Polystyrene sulfonate
SEM	Scanning Electron microscopy
SPR	Surface plasmon resonance
SR	Starch
TEM	Transmission electron microscopy
tMSPm	(Trimethoxysilyl) propyl methacrylate
UV/Vis	Ultraviolet/Visible
Vac	Vinyl acetic acid
VC	N-vinylcaprolactam
VP	Vinyl pyrrolidone
VPTT	Volume phase transition temperature
XRD	X-ray diffraction
2-NA	2-nitroaniline
2-AA	2-aminoaniline
4-NA	4-nitroaniline

## Acknowledgments

Authors are grateful to Higher Education Commission Pakistan for financial support under National Research Program for Universities (NRPU) [No.20-3995/NRPU/R&D/HEC/14/1212], Pakistan Program for Collaborative Research (PPCR) [22-3/HEC/R&D/PPCR/2018] and University of the Punjab under research grant for the fiscal year 2017-2018 to carry out this study. Ahmad Irfan would like to express his gratitude to Research Center for Advanced Materials Science, King Khalid University, Abha, Saudi Arabia for support.

## ORCID

Zahoor H. Farooqi  <http://orcid.org/0000-0003-3200-2935>

## References

- [1] Han, J.; Wang, M.; Hu, Y.; Zhou, C.; Guo, R. Conducting Polymer-Noble Metal Nanoparticle Hybrids: Synthesis Mechanism Application. *Prog. Polym. Sci.* **2017**, *70*, 52–91. DOI: 10.1016/j.progpolymsci.2017.04.002.
- [2] Khan, Z. U. H.; Khan, A.; Chen, Y. M.; Shah, N. S.; Muhammad, N.; Khan, A. U.; Tahir, K.; Khan, F. U.; Murtaza, B.; Hassan, S. U. Biomedical Applications of Green Synthesized Nobel Metal Nanoparticles. *J. Photochem. Photobiol.* **2017**, *173*, 150–164. DOI: 10.1016/j.jphotobiol.2017.05.034.
- [3] Xu, P.; Han, X.; Zhang, B.; Du, Y.; Wang, H.-L. Multifunctional Polymer-Metal Nanocomposites via Direct Chemical Reduction by Conjugated Polymers. *Chem. Soc. Rev.* **2014**, *43*, 1349–1360. DOI: 10.1039/C3CS60380F.
- [4] Prakash, J.; Pivin, J.; Swart, H. Noble Metal Nanoparticles Embedding into Polymeric Materials: From Fundamentals to Applications. *Adv. Colloid. Interface Sci.* **2015**, *226*, 187–202. DOI: 10.1016/j.cis.2015.10.010.
- [5] Farooqi, Z. H.; Khan, S. R.; Hussain, T.; Begum, R.; Ejaz, K.; Majeed, S.; Ajmal, M.; Kanwal, F.; Siddiq, M. Effect of Crosslinker Feed Content on Catalytic Activity of Silver Nanoparticles Fabricated in Multiresponsive Microgels. *Korean J. Chem. Eng.* **2014**, *31*, 1674–1680. DOI: 10.1007/s11814-014-0117-0.
- [6] Gorelikov, I.; Field, L. M.; Kumacheva, E. Hybrid Microgels Photoresponsive in the Near-Infrared Spectral Range. *J. Am. Chem. Soc.* **2004**, *126*, 15938–15939. DOI: 10.1021/ja0448869.
- [7] Naseem, K.; Begum, R.; Wu, W.; Irfan, A.; Farooqi, Z. H. Advancement in Multi-Functional Poly (styrene)-Poly (N-isopropylacrylamide) Based Core-Shell Microgels and their Applications. *Polym. Rev.* **2018**, *1*–38. DOI: 10.1080/15583724.2017.1423326. In press.
- [8] Farooqi, Z. H.; Khalid, R.; Begum, R.; Farooq, U.; Wu, Q.; Wu, W.; Ajmal, M.; Irfan, A.; Naseem, K. Facile Synthesis of Silver Nanoparticles in a Crosslinked Polymeric System by in Situ Reduction Method for Catalytic Reduction of 4-nitroaniline. *Environ. Technol.* **2018**. DOI: 10.1080/09593330.2018.1435737.
- [9] Liz-Marzán, L. M.; Lado-Tourinho, I. Reduction and Stabilization of Silver Nanoparticles in Ethanol by Nonionic Surfactants. *Langmuir.* **1996**, *12*, 3585–3589. DOI: 10.1021/la951501e.
- [10] Niu, Y.; Crooks, R. M. Preparation of Dendrimer-Encapsulated Metal Nanoparticles Using Organic Solvents. *Chem. Mater.* **2003**, *15*, 3463–3467. DOI: 10.1021/cm034172h.
- [11] Sakai, T.; Alexandridis, P. Single-Step Synthesis and Stabilization of Metal Nanoparticles in Aqueous Pluronic Block Copolymer Solutions at Ambient Temperature. *Langmuir.* **2004**, *20*, 8426–8430. DOI: 10.1021/la049514s.
- [12] Farooqi, Z. H.; Naseem, K.; Ijaz, A.; Begum, R. Engineering of Silver Nanoparticle Fabricated Poly(N-isopropylacrylamide-co-acrylic acid) Microgels for Rapid Catalytic Reduction of Nitrobenzene. *J. Polym. Eng.* **2016**, *36*, 87–96. DOI: 10.1515/polyeng-2015-0082.
- [13] Begum, R.; Naseem, K.; Farooqi, Z. H. A Review of Responsive Hybrid Microgels Fabricated with Silver Nanoparticles: Synthesis, Classification, Characterization and Applications. *J. Sol-Gel Sci. Technol.* **2016**, *77*, 497–515. DOI: 10.1007/s10971-015-3896-9.
- [14] Wu, W.; Shen, J.; Banerjee, P.; Zhou, S. Chitosan-based Responsive Hybrid Nanogels for Integration of Optical pH-sensing, Tumor Cell Imaging and Controlled Drug Delivery. *Biomaterials.* **2010**, *31*, 8371–8381. DOI: 10.1016/j.biomaterials.2010.07.061.
- [15] Wu, W.; Zhou, T.; Shen, J.; Zhou, S. Optical Detection of Glucose by CdS Quantum Dots Immobilized in Smart Microgels. *Chem. Commun.* **2009**, 4390–4392. DOI: 10.1039/b907348e.
- [16] Thomas, V.; Namdeo, M.; Murali Mohan, Y.; Bajpai, S.; Bajpai, M. Review on Polymer, Hydrogel and Microgel Metal Nanocomposites: A Facile Nanotechnological Approach. *J. Macromol. Sci. A.* **2007**, *45*, 107–119. DOI: 10.1080/10601320701683470.

- [17] Xu, S.; Zhang, J.; Paquet, C.; Lin, Y.; Kumacheva, E. From Hybrid Microgels to Photonic Crystals. *Adv. Funct. Mater.* **2003**, *13*, 468–472. DOI: 10.1002/adfm.200304338.
- [18] Naseer, F.; Ajmal, M.; Bibi, F.; Farooqi, Z. H.; Siddiq, M. Copper and Cobalt Nanoparticles Containing Poly (acrylic acid-co-acrylamide) Hydrogel Composites for Rapid Reduction of 4-Nitrophenol and Fast Removal of Malachite Green from Aqueous Medium. *Polym. Compos.* **2017**. DOI: 10.1002/pc.24329.
- [19] Farooqi, Z. H.; Ijaz, A.; Begum, R.; Naseem, K.; Usman, M.; Ajmal, M.; Saeed, U. Synthesis and Characterization of Inorganic–organic Polymer Microgels for Catalytic Reduction of 4-Nitroaniline in Aqueous Medium. *Polym. Compos.* **2016**, *39*, 645–653.
- [20] Lu, Y.; Mei, Y.; Ballauff, M.; Drechsler, M. Thermosensitive Core–shell Particles as Carrier Systems for Metallic Nanoparticles. *J. Phys. Chem. B.* **2006**, *110*, 3930–3937. DOI: 10.1021/jp057149n.
- [21] Contreras-Cáceres, R.; Pacifico, J.; Pastoriza-Santos, I.; Pérez-Juste, J.; Fernández-Barbero, A.; Liz-Marzán, L. M. Au@pNIPAM Thermosensitive Nanostructures: Control over Shell Cross-linking, Overall Dimensions, and Core Growth. *Adv. Funct. Mater.* **2009**, *19*, 3070–3076. DOI: 10.1002/adfm.200900481.
- [22] Wagner, T.; Nedilko, A.; Linn, M.; Chigrin, D. N.; von Plessen, G.; Böker, A. Controlled Gold Nanorod Reorientation and Hexagonal Order in Micromolded Gold Nanorod@pNIPAM Microgel Chain Arrays. *Small* **2017**, *13*, 1603054–1603063. DOI: 10.1002/smll.201603054.
- [23] Hellweg, T.; Dewhurst, C. D.; Eimer, W.; Kratz, K. PNIPAm-Co-Polystyrene Core–Shell Microgels: Structure, Swelling Behavior, and Crystallization. *Langmuir* **2004**, *20*, 4330–4335. DOI: 10.1021/la0354786.
- [24] Farooqi, Z. H.; Naseem, K.; Begum, R.; Ijaz, A. Catalytic Reduction of 2-nitroaniline in Aqueous Medium Using Silver Nanoparticles Functionalized Polymer Microgels. *J. Inorg. Organomet. Polym. Mater.* **2015**, *25*, 1554–1568. DOI: 10.1007/s10904-015-0275-5.
- [25] Yang, L.-Q.; Hao, M.-M.; Wang, H.-Y.; Zhang, Y. Amphiphilic Polymer-Ag Composite Microgels with Tunable Catalytic Activity and Selectivity. *Colloid Polym. Sci.* **2015**, *293*, 2405–2417. DOI: 10.1007/s00396-015-3642-4.
- [26] Zhang, J. T.; Wei, G.; Keller, T. F.; Gallagher, H.; Stötzel, C.; Müller, F. A.; Gottschaldt, M.; Schubert, U. S.; Jandt, K. D. Responsive Hybrid Polymeric/Metallic Nanoparticles for Catalytic Applications. *Macromol. Mater. Eng.* **2010**, *295*, 1049–1057. DOI: 10.1002/mame.201000204.
- [27] Wang, Q.; Zhao, Y.; Xu, H.; Yang, X.; Yang, Y. Thermosensitive Phase Transition Kinetics of Poly(N-Isopropylacryl Amide-co-Acrylamide) Microgel Aqueous Dispersions. *J. Appl. Polym. Sci.* **2009**, *113*, 321–326. DOI: 10.1002/app.29642.
- [28] Naseem, K.; Ur Rehman, M. A.; Huma, R. Review on Vinyl Acetic Acid-based Polymer Microgels for Biomedical and Other Applications. *Int. J. Polym. Mater.* **2018**, *67*, 322–332. DOI: 10.1080/00914037.2017.1327434.
- [29] Najeeb, J.; Ahmad, G.; Nazir, S.; Naseem, K.; Kanwal, A. Critical Analysis of Various Supporting Mediums Employed for the Incapacitation of Silver Nanomaterial for Aniline and Phenolic Pollutants: A Review. *Korean J. Chem. Eng.* **2017**. DOI: 10.1007/s11814-017-0192-0.
- [30] Naseem, K.; Begum, R.; Farooqi, Z. H. Platinum Nanoparticles Fabricated Multiresponsive Microgel Composites: Synthesis, Characterization, and Applications. *Polym. Compos.* **2016**. DOI: 10.1002/pc.24212.
- [31] Das, M.; Sanson, N.; Fava, D.; Kumacheva, E. Microgels Loaded with Gold Nanorods: Photothermally Triggered Volume Transitions under Physiological Conditions. *Langmuir* **2007**, *23*, 196–201. DOI: 10.1021/la061596s.
- [32] Khan, A.; El-Toni, A. M.; Alrokayan, S.; Alsahhi, M.; Alhoshan, M.; Aldwayyan, A. S. Microwave-Assisted Synthesis of Silver Nanoparticles Using Poly-N-Isopropylacrylamide/Acrylic Acid Microgel Particles. *Colloids Surf., A.* **2011**, *377*, 356–360. DOI: 10.1016/j.colsurfa.2011.01.042.
- [33] Volden, S.; Eilertsen, J. L.; Singh, G.; Wang, W.; Zhu, K.; Nyström, B.; Glomm, W. R. Effect of Charge Density Matching on the Temperature Response of PNIPAAm Block Copolymer–Gold Nanoparticles. *J. Phys. Chem. C.* **2012**, *116*, 12844–12853. DOI: 10.1021/jp300754b.
- [34] Zhang, J.; Xu, S.; Kumacheva, E. Polymer Microgels: Reactors for Semiconductor, Metal, and Magnetic Nanoparticles. *J. Am. Chem. Soc.* **2004**, *126*, 7908–7914. DOI: 10.1021/ja031523k.
- [35] Lu, Y.; Mei, Y.; Drechsler, M.; Ballauff, M. Thermosensitive Core-shell Particles as Carriers for Ag Nanoparticles: Modulating the Catalytic Activity by a Phase Transition in Networks. *Angew. Chem. Int. Ed.* **2006**, *45*, 813–816. DOI: 10.1002/anie.200502731.
- [36] Suzuki, D.; McGrath, J. G.; Kawaguchi, H.; Lyon, L. A. Colloidal Crystals of Thermosensitive, Core/shell Hybrid Microgels. *J. Phys. Chem. C.* **2007**, *111*, 5667–5672. DOI: 10.1021/jp068535n.
- [37] Contreras-Cáceres, R.; Pastoriza-Santos, I.; Alvarez-Puebla, R. A.; Pérez-Juste, J.; Fernández-Barbero, A.; Liz-Marzán, L. M. Growing Au/Ag Nanoparticles within Microgel Colloids for Improved Surface-Enhanced Raman Scattering Detection. *Chem. Eur. J.* **2010**, *16*, 9462–9467. DOI: 10.1002/chem.201001261.
- [38] Suzuki, D.; Kawaguchi, H. Modification of Gold Nanoparticle Composite Nanostructures Using Thermosensitive Core–Shell Particles as a Template. *Langmuir* **2005**, *21*, 8175–8179. DOI: 10.1021/la0504356.
- [39] Kim, J.-H.; Lee, T. R. Hydrogel-Templated Growth of Large Gold Nanoparticles: Synthesis of Thermally Responsive Hydrogel–Nanoparticle Composites. *Langmuir* **2007**, *23*, 6504–6509. DOI: 10.1021/la0629173.
- [40] Contreras-Cáceres, R.; Sánchez-Iglesias, A.; Karg, M.; Pastoriza-Santos, I.; Pérez-Juste, J.; Pacifico, J.; Hellweg, T.; Fernández-Barbero, A.; Liz-Marzán, L. M. Encapsulation and Growth of Gold Nanoparticles in Thermoresponsive Microgels. *Adv. Mater.* **2008**, *20*, 1666–1670. DOI: 10.1002/adma.200800064.
- [41] Zhang, J.; Xu, S.; Kumacheva, E. Photogeneration of Fluorescent Silver Nanoclusters in Polymer Microgels. *Adv. Mater.* **2005**, *17*, 2336–2340. DOI: 10.1002/adma.200501062.
- [42] Wu, Z.; Chen, X.; Li, J.-Y.; Pan, C.-Y.; Hong, C.-Y. Au–Polymer Hybrid Microgels Easily Prepared by Thermo-Induced Self-Cross-linking and In Situ Reduction. *RSC Adv.* **2016**, *6*, 48927–48932. DOI: 10.1039/C6RA07864H.
- [43] Wu, W.; Zhou, T.; Zhou, S. Tunable Photoluminescence of Ag Nanocrystals in Multiple-Sensitive Hybrid Microgels. *Chem. Mater.* **2009**, *21*, 2851–2861. DOI: 10.1021/cm900635u.
- [44] Fernández-López, C.; Pérez-Balado, C.; Pérez-Juste, J.; Pastoriza-Santos, I.; de Lera, Á. R.; Liz-Marzán, L. M. A General LbL Strategy for the Growth of pNIPAM Microgels on Au Nanoparticles with Arbitrary Shapes. *Soft Matter* **2012**, *8*, 4165–4170. DOI: 10.1039/C1SM06396K.
- [45] Pastoriza-Santos, I.; Pérez-Juste, J.; Liz-Marzán, L. M. Silica-Coating and Hydrophobation of CTAB-Stabilized Gold Nanorods. *Chem. Mater.* **2006**, *18*, 2465–2467. DOI: 10.1021/cm060293g.
- [46] Dong, Y.; Ma, Y.; Zhai, T.; Shen, F.; Zeng, Y.; Fu, H.; Yao, J. Silver Nanoparticles Stabilized by Thermoresponsive Microgel Particles: Synthesis and Evidence of an Electron Donor–Acceptor Effect. *Macromol. Rapid Commun.* **2007**, *28*, 2339–2345. DOI: 10.1002/marc.200700483.
- [47] Begum, R.; Farooqi, Z. H.; Ahmed, E.; Naseem, K.; Ashraf, S.; Sharif, A.; Rehan, R. Catalytic Reduction of 4-Nitrophenol Using Silver Nanoparticles-Engineered Poly (N-isopropylacrylamide-co-acrylamide) Hybrid Microgels. *Appl. Organomet. Chem.* **2017**, *31*, 3563–3571. DOI: 10.1002/aoc.3563.
- [48] Tang, Y.; Wu, T.; Hu, B.; Yang, Q.; Liu, L.; Yu, B.; Ding, Y.; Ye, S. Synthesis of Thermo- and pH-responsive Ag Nanoparticle-Embedded Hybrid Microgels and their Catalytic Activity in Methylene Blue Reduction. *Mater. Chem. Phys.* **2015**, *149*, 460–466. DOI: 10.1016/j.matchemphys.2014.10.045.
- [49] Khan, S. R.; Farooqi, Z. H.; Ajmal, M.; Siddiq, M.; Khan, A. Synthesis, Characterization, and Silver Nanoparticles Fabrication in N-isopropylacrylamide-Based Polymer Microgels for Rapid Degradation of p-Nitrophenol. *J. Dispersion Sci. Technol.* **2013**, *34*, 1324–1333. DOI: 10.1080/01932691.2012.744690.
- [50] Wu, W.; Zhou, T.; Berliner, A.; Banerjee, P.; Zhou, S. Smart Core–Shell Hybrid Nanogels with Ag Nanoparticle Core for Cancer Cell

- Imaging and Gel Shell for pH-Regulated Drug Delivery. *Chem. Mater.* **2010**, *22*, 1966–1976. DOI: 10.1021/cm903357q.
- [51] Ajmal, M.; Farooqi, Z. H.; Siddiq, M. Silver Nanoparticles Containing Hybrid Polymer Microgels with Tunable Surface Plasmon Resonance and Catalytic Activity. *Korean J. Chem. Eng.* **2013**, *30*, 2030–2036. DOI: 10.1007/s11814-013-0150-4.
- [52] Farooqi, Z. H.; Siddiq, M. Temperature-Responsive Poly (N-Isopropylacrylamide-Acrylamide-Phenylboronic Acid) Microgels for Stabilization of Silver Nanoparticles. *J. Dispersion Sci. Technol.* **2015**, *36*, 423–429. DOI: 10.1080/01932691.2014.911106.
- [53] Shah, L. A.; Ambreen, J.; Bibi, I.; Sayed, M.; Siddiq, M. Silver Nanoparticles Fabricated Hybrid Microgels for Optical and Catalytic Study. *J. Chem. Soc. Pak.* **2016**, *38*, 850–858.
- [54] Suzuki, D.; Kawaguchi, H. Hybrid Microgels with Reversibly Changeable Multiple Brilliant Color. *Langmuir.* **2006**, *22*, 3818–3822. DOI: 10.1021/la052999f.
- [55] Ur Rehman, S.; Khan, A. R.; Shah, A.; Badshah, A.; Siddiq, M. Preparation and Characterization of Poly (N-Isopropylacrylamide-Dimethylaminoethyl Methacrylate) Microgels and their Composites of Gold Nanoparticles. *Colloids Surf., A.* **2017**, *520*, 826–833. DOI: 10.1016/j.colsurfa.2017.02.060.
- [56] Shah, L. A.; Sayed, M.; Fayaz, M.; Bibi, I.; Nawaz, M.; Siddiq, M. Ag-loaded Thermo-sensitive Composite Microgels for Enhanced Catalytic Reduction of Methylene Blue. *Nanotechnol. Environ. Eng.* **2017**, *2*, 1–14. DOI: 10.1007/s41204-017-0026-7.
- [57] Lu, Y.; Proch, S.; Schrinner, M.; Drechsler, M.; Kempe, R.; Ballauff, M. Thermosensitive Core-shell Microgel as a “Nanoreactor” for Catalytic Active Metal Nanoparticles. *J. Mater. Chem.* **2009**, *19*, 3955–3961. DOI: 10.1039/b822673n.
- [58] Farooqi, Z. H.; Khan, S. R.; Begum, R.; Kanwal, F.; Sharif, A.; Ahmed, E.; Majeed, S.; Ejaz, K.; Ijaz, A. Effect of Acrylic Acid Feed Contents of Microgels on Catalytic Activity of Silver Nanoparticles Fabricated Hybrid Microgels. *Turk. J. Chem.* **2015**, *39*, 96–107. DOI: 10.3906/kim-1406-40.
- [59] Suzuki, D.; Kawaguchi, H. Gold Nanoparticle Localization at the Core Surface by Using Thermosensitive Core-Shell Particles as a Template. *Langmuir.* **2005**, *21*, 12016–12024. DOI: 10.1021/la0516882.
- [60] Vimala, K.; Sivudu, K. S.; Mohan, Y. M.; Sreedhar, B.; Raju, K. M. Controlled Silver Nanoparticles Synthesis in Semi-hydrogel Networks of Poly (Acrylamide) and Carbohydrates: A Rational Methodology for Antibacterial Application. *Carbohydr. Polym.* **2009**, *75*, 463–471. DOI: 10.1016/j.carbpol.2008.08.009.
- [61] Karg, M.; Pastoriza-Santos, I.; Pérez-Juste, J.; Hellweg, T.; Liz-Marzán, L. M. Nanorod-Coated PNIPAM Microgels: Thermoresponsive Optical Properties. *Small.* **2007**, *3*, 1222–1229. DOI: 10.1002/smll.200700078.
- [62] Das, M.; Mordoukhovskii, L.; Kumacheva, E. Sequestering Gold Nanorods by Polymer Microgels. *Adv. Mater.* **2008**, *20*, 2371–2375. DOI: 10.1002/adma.200702860.
- [63] Lu, Y.; Yuan, J.; Polzer, F.; Drechsler, M.; Preussner, J. In Situ Growth of Catalytic Active Au–Pt Bimetallic Nanorods in Thermoresponsive Core-Shell Microgels. *ACS Nano.* **2010**, *4*, 7078–7086. DOI: 10.1021/nn102622d.
- [64] Rodríguez-Fernández, J.; Fedoruk, M.; Hrelescu, C.; Lutich, A. A.; Feldmann, J. Triggering the Volume Phase Transition of Core-shell Au Nanorod-Microgel Nanocomposites with Light. *Nanotechnology.* **2011**, *22*, 245708–245716. DOI: 10.1088/0957-4484/22/24/245708.
- [65] Kawano, T.; Niidome, Y.; Mori, T.; Katayama, Y.; Niidome, T. PNIPAM gel-Coated Gold Nanorods for Targeted Delivery Responding to a Near-infrared Laser. *Bioconjugate Chem.* **2009**, *20*, 209–212. DOI: 10.1021/bc800480k.
- [66] Khan, A. Preparation and Characterization of N-isopropylacrylamide/Acrylic Acid Copolymer Core-Shell Microgel Particles. *Colloid Interface Sci.* **2007**, *313*, 697–704. DOI: 10.1016/j.cis.2007.05.027.
- [67] Wang, Y.; Wei, G.; Wen, F.; Zhang, X.; Zhang, W.; Shi, L. Synthesis of Gold Nanoparticles Stabilized with Poly(N-Isopropylacrylamide)-co-poly (4-Vinyl Pyridine) Colloid and Their Application in Responsive Catalysis. *J. Mol. Catal. A: Chem.* **2008**, *280*, 1–6. DOI: 10.1016/j.molcata.2007.10.014.
- [68] Fundueanu, G.; Constantin, M.; Ascenzi, P. Poly(N-isopropylacrylamide-co-Acrylamide) Cross-linked Thermoresponsive Microspheres Obtained from Preformed Polymers: Influence of the Physico-Chemical Characteristics of Drugs on their Release Profiles. *Acta Biomater.* **2009**, *5*, 363–373. DOI: 10.1016/j.actbio.2008.07.011.
- [69] Fundueanu, G.; Constantin, M.; Ascenzi, P. Fast-Responsive Porous Thermoresponsive Microspheres for Controlled Delivery of Macromolecules. *Int. J. Pharm.* **2009**, *379*, 9–17. DOI: 10.1016/j.ijpharm.2009.05.064.
- [70] Ajmal, M.; Demirci, S.; Siddiq, M.; Aktas, N.; Sahiner, N. Simultaneous Catalytic Degradation/reduction of Multiple Organic Compounds by Modifiable p(methacrylic acid-co-acrylonitrile)-M (M: Cu, Co) Microgel Catalyst Composites. *New J. Chem.* **2016**, *40*, 1485–1496. DOI: 10.1039/C5NJ02298C.
- [71] Khan, S. R.; Farooqi, Z. H.; Ali, A.; Begum, R.; Kanwal, F.; Siddiq, M. Kinetics and Mechanism of Reduction of Nitrobenzene Catalyzed by Silver-poly(N-Isopropylacrylamide-co-Allylactic Acid) Hybrid Microgels. *Mater. Chem. Phys.* **2016**, *171*, 318–327. DOI: 10.1016/j.matchemphys.2016.01.023.
- [72] Shah, L. A.; Haleem, A.; Sayed, M.; Siddiq, M. Synthesis of Sensitive Hybrid Polymer Microgels for Catalytic Reduction of Organic Pollutants. *J. Environ. Chem. Eng.* **2016**, *4*, 3492–3497. DOI: 10.1016/j.jece.2016.07.029.
- [73] Liu, Y.-Y.; Liu, X.-Y.; Yang, J.-M.; Lin, D.-L.; Chen, X.; Zha, L.-S. Investigation of Ag Nanoparticles Loading Temperature Responsive Hybrid Microgels and their Temperature Controlled Catalytic Activity. *Colloids Surf., A.* **2012**, *393*, 105–110. DOI: 10.1016/j.colsurfa.2011.11.007.
- [74] Pich, A.; Karak, A.; Lu, Y.; Ghosh, A. K.; Adler, H.-J. P. Tuneable Catalytic Properties of Hybrid Microgels Containing Gold Nanoparticles. *J. Nanosci. Nanotechnol.* **2006**, *6*, 3763–3769. DOI: 10.1166/jnn.2006.621.
- [75] Wu, S.; Dzubiella, J.; Kaiser, J.; Drechsler, M.; Guo, X.; Ballauff, M.; Lu, Y. Thermosensitive Au–PNIPAA Yolk-Shell Nanoparticles with Tunable Selectivity for Catalysis. *Angew. Chem. Int. Ed.* **2012**, *51*, 2229–2233. DOI: 10.1002/anie.201106515.
- [76] Mei, Y.; Lu, Y.; Polzer, F.; Ballauff, M.; Drechsler, M. Catalytic Activity of Palladium Nanoparticles Encapsulated in Spherical Polyelectrolyte Brushes and Core-shell Microgels. *Chem. Mater.* **2007**, *19*, 1062–1069. DOI: 10.1021/cm062554s.
- [77] Cho, S.; Li, Y.; Seo, M.; Kumacheva, E. Nanofibrillar Stimulus-Responsive Cholesteric Microgels with Catalytic Properties. *Angew. Chem. Int. Ed.* **2016**, *55*, 14014–14018. DOI: 10.1002/anie.201607406.
- [78] Naseem, K.; Begum, R.; Farooqi, Z. H. Catalytic Reduction of 2-Nitroaniline: a Review. *Environ. Sci. Pollut. Res.* **2017**, *24*, 6446–6460. DOI: 10.1007/s11356-016-8317-2.
- [79] Wang, L.; Chen, S.; Zhou, J.; Yang, J.; Chen, X.; Ji, Y.; Liu, X.; Zha, L. Silver Nanoparticles Loaded Thermoresponsive Hybrid Nanofibrous Hydrogel as a Recyclable Dip-Catalyst with Temperature-Tunable Catalytic Activity. *Macromol. Mater. Eng.* **2017**, *302*, 1700181–1700189. DOI: 10.1002/mame.201700181.
- [80] Zhang, C.; Li, C.; Chen, Y.; Zhang, Y. Synthesis and Catalysis of Ag Nanoparticles Trapped into Temperature-Sensitive and Conductive Polymers. *J. Mater. Sci.* **2014**, *49*, 6872–6882. DOI: 10.1007/s10853-014-8389-7.
- [81] Farooqi, Z. H.; Iqbal, S.; Khan, S. R.; Kanwal, F.; Begum, R. Cobalt and Nickel Nanoparticles Fabricated p (NIPAM-co-MAA) Microgels for Catalytic Applications. *e-Polymers.* **2014**, *14*, 313–321. DOI: 10.1515/epoly-2014-0111.
- [82] Ajmal, M.; Demirci, S.; Siddiq, M.; Aktas, N.; Sahiner, N. Betaine Microgel Preparation from 2-(methacryloyloxy ethyl) dimethyl (3-sulfopropyl) Ammonium Hydroxide and Its Use as a Catalyst System. *Colloids Surf., A.* **2015**, *486*, 29–37. DOI: 10.1016/j.colsurfa.2015.09.028.